

# Journal of Biomedical Optics

[SPIDigitalLibrary.org/jbo](http://SPIDigitalLibrary.org/jbo)

## **Reflectance model for acetowhite epithelium**

George Zonios



**SPIE**

# Reflectance model for acetowhite epithelium

George Zonios

University of Ioannina, Department of Materials Science and Engineering, 45110 Ioannina, Greece

**Abstract.** Application of low concentration acetic acid solution to various types of human epithelia, *in vivo*, is a well-established technique for the visual identification of neoplastic and potential precancerous lesions, especially in the cervix. An acetic acid application produces a transient whitening effect associated with the aforementioned lesions (acetowhite effect). In this article, a simple semi-empirical tissue reflectance model is presented, which describes the acetowhite effect in terms of the tissue's optical properties and layered structure. The model successfully describes data available in the literature, explains basic characteristics of the acetowhite effect, and can serve as the basis for the development of more accurate and reliable noninvasive diagnostic methodologies for precancerous epithelial lesions. © 2012 Society of Photo-Optical Instrumentation Engineers (SPIE). [DOI: 10.1117/1.JBO.17.8.087003]

Keywords: reflectance; multiple scattering; spectroscopy.

Paper 12286 received May 8, 2012; revised manuscript received Jun. 26, 2012; accepted for publication Jul. 10, 2012; published online Sep. 4, 2012.

## 1 Introduction

Acetic acid is routinely used for the *in vivo* clinical examination of various types of epithelial tissues.<sup>1,2</sup> Topical application of dilute solution (3% to 5%) of acetic acid causes a transient whitening effect (acetowhite effect) in neoplastic and precancerous epithelial lesions that facilitates their visual detection and identification. The technique is widely used for the routine screening of cervical neoplasia using colposcopy.<sup>1–10</sup> In the cervix, neoplasia [cervical intraepithelial neoplasia (CIN)] is classified in three grades: CIN grade 1, CIN grade 2, and CIN grade 3. CIN1 (low grade) is generally considered a benign condition that may disappear by itself, while grades CIN2 and CIN3 (high grade) represent potential precancerous lesions. Figure 1 illustrates the morphology of the cervical epithelium with an average thickness of 0.36 mm and typical thickness variation in the 0.2 to 0.5 mm range.<sup>11</sup> Dysplastic cells are generally present in the bottom one-third of the epithelium in CIN1, in the bottom two thirds in CIN2, and throughout the entire epithelium in CIN3.

The acetowhite effect typically lasts for a few minutes and is caused by changes in the optical properties of the dysplastic epithelium, which are induced by acetic acid. Even though the exact mechanism underlying the changes in the optical properties is not known, it is believed to be due to a temporary increase in the scattering properties of the dysplastic epithelium caused by the acetic acid.<sup>5,6</sup> In this article, a reflectance model for the acetowhite effect is presented for the first time (to the author's knowledge) in terms of tissue optical properties and morphological characteristics. The model is quite successful in describing experimental observations already reported in the literature by other researchers<sup>4–10</sup> and in explaining key characteristics of the acetowhite effect. In that sense, it is very promising for the further understanding of the effect, as well as for the development of quantitative diagnostic algorithms and tools for the reliable noninvasive detection and characterization of precancerous epithelial lesions.

## 2 Methods

### 2.1 Monte Carlo Simulations

Monte Carlo (MC) simulations of light propagation in biological tissue were performed using the MCML code.<sup>12</sup> Each MC simulation was performed with one million photons incident in a perpendicular infinitely thin beam configuration. The simulated cervical epithelium morphology is presented in Fig. 1. A two-layer semi-infinite tissue model was assumed to simulate CIN3 with the top layer corresponding to the epithelium layer and the bottom layer corresponding to the stroma layer. Table 1 summarizes the parameters used in the simulations for CIN3. As shown, the reduced-scattering coefficient in the epithelium layer was varied to simulate the acetowhite effect. To simulate CIN1 and CIN2 morphology, a three-layer tissue geometry was employed with the top two layers simulating the epithelium and the bottom layer simulating the stroma (Fig. 1 and Tables 2 and 3). Reflectance was measured up to a distance of 20 mm away from the incident beam at an exit angle range of 0 deg to 30 deg with respect to the vertical on the tissue surface, so as to better simulate a typical imaging geometry for cervix colposcopy using a CCD camera, as reported elsewhere.<sup>6</sup> Reflectance normalization was performed by simulating a highly scattering material ( $\mu'_s = 100 \text{ mm}^{-1}$  and  $\mu_a = 0.001 \text{ mm}^{-1}$ ), again to better simulate the reflectance normalization used in Ref. 6. The scattering anisotropy coefficient of tissue was assumed  $g = 0.9$  (Heaney-Greenstein scattering phase function<sup>12</sup>) and the refractive index was assumed equal to 1.4. Optical property values included in Tables 1 to 3 are typical for soft epithelial tissues, such as the human cervical epithelium, in the visible and near-infrared spectral regions.<sup>13</sup>

### 2.2 Data Analysis

Fitting to the MC data was performed using the TableCurve2D software package (Systat) that utilized the Levenberg—Marquardt minimization method. By feeding the data into a library of numerous trial functions and categorizing the results

Address all correspondence to: George Zonios, University of Ioannina, Department of Materials Science and Engineering, 45110 Ioannina, Greece. Tel: +302651007228; E-mail: gzonios@cc.uoi.gr.

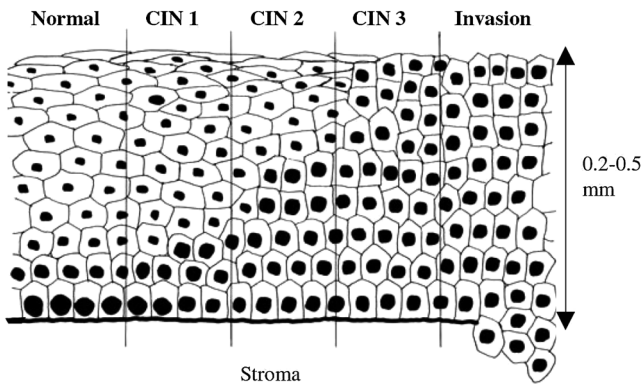


Fig. 1 Morphology of cervical squamous cell epithelium and progression stages of CIN (reproduced from Ref. 11, with permission).

according to the most appropriate fit, TableCurve2D enabled the identification of the simplest empirical functions for the description of the data. The exact form of the empirical Eqs. (2) and (3) were determined this way.

### 3 Results

CIN3 lesions can be modeled by employing a two-layer geometry and thus are presented first. Figure 2 shows results from the simulations of CIN3 cervix lesions using the parameter values of Table 1. The most important observation here is that reflectance strongly depends on the absorption coefficient of the stroma layer. If stroma absorption is significant, then significant changes in the reflectance are observed as a result of changes in the reduced-scattering coefficient of the epithelium layer. On the other hand, if stroma absorption is low, this causes changes in the reduced-scattering coefficient of the epithelium layer to have little effect in the total reflectance observed and, as a result,

Table 1 Simulation parameters for CIN3.

Layer	Thickness (mm)	$\mu_{\alpha}$ (mm <sup>-1</sup> )	$\mu'_s$ (mm <sup>-1</sup> )
Top layer (epithelium—acetowhite effect)			1.0
			1.5
			2.0
			3.0
		0.20	4.0
		0.28	6.0
		0.36	8.0
		0.50	10.0
			12.0
			14.0
Bottom layer (stroma)		0.005	
		0.010	
		0.025	
		0.050	1.0
		0.100	1.6
	1000	0.250	2.0
		0.500	
		1.000	
		2.500	
		5.000	

Table 2 Simulation parameters for CIN1.

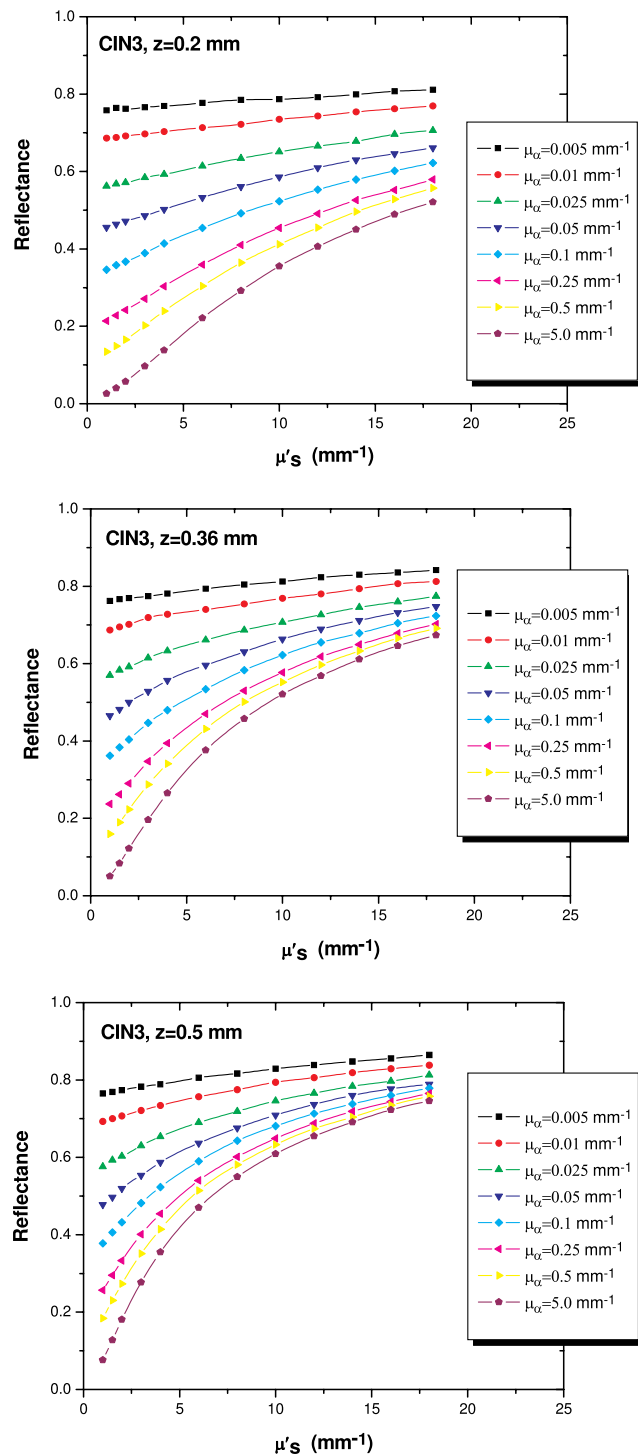
Layer	Thickness (mm)	$\mu_{\alpha}$ (mm <sup>-1</sup> )	$\mu'_s$ (mm <sup>-1</sup> )
First layer (epithelium—no acetowhite effect)	0.24	0	1.0
Second layer (epithelium—acetowhite effect)			1.0
			1.5
			2.0
			3.0
		0.12	0
			6.0
			8.0
			10.0
			12.0
			14.0
Bottom layer (stroma)		0.005	
		0.010	
		0.025	
		0.050	1.0
		0.100	1.6
	1000	0.250	2.0
		0.500	
		1.000	
		2.500	
		5.000	

**Table 3** Simulation parameters for CIN2.

Layer	Thickness (mm)	$\mu_a$ ( $\text{mm}^{-1}$ )	$\mu'_s$ ( $\text{mm}^{-1}$ )
First layer (epithelium—no acetowhite effect)	0.12	0	1.0
			1.0
			1.5
			2.0
			3.0
			4.0
			6.0
			10.0
			12.0
			14.0
Second layer (epithelium—acetowhite effect)	0.24	0	0.005
			0.010
			0.025
			0.050
			0.100
Bottom layer (stroma)	1000	1.6	0.250
			0.500
			1.000
			2.500
			5.000

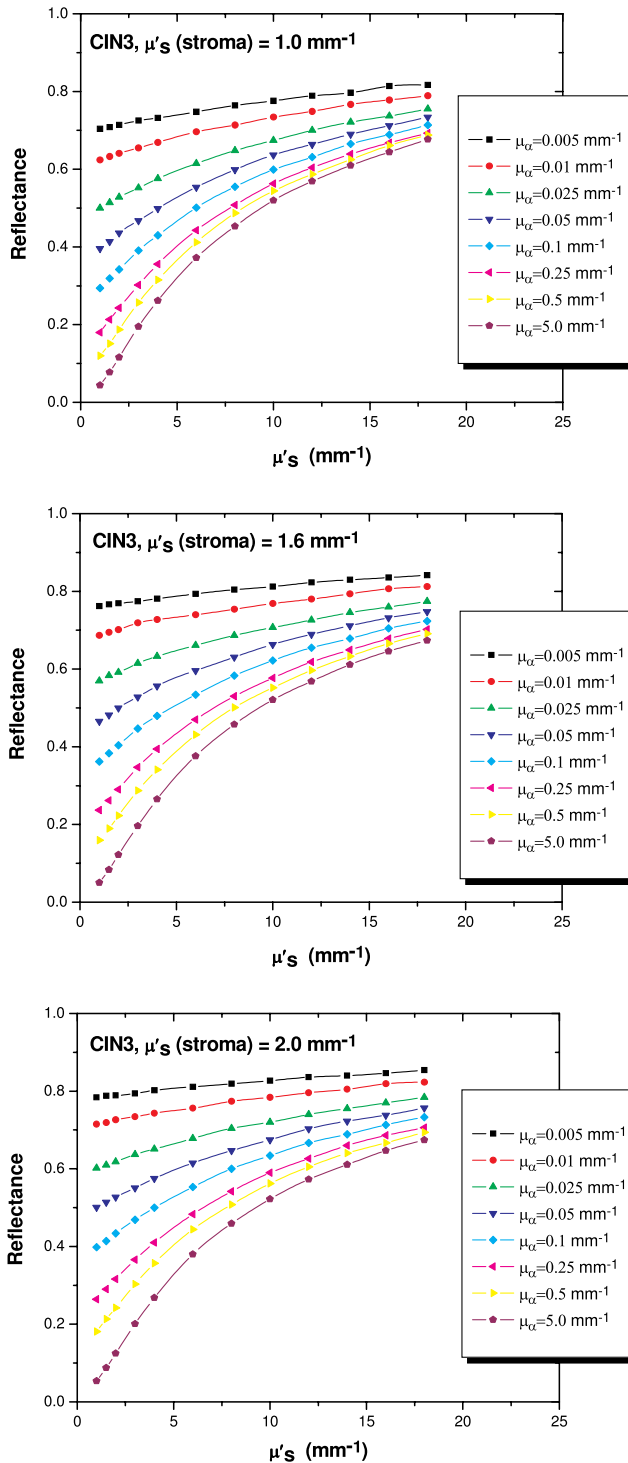
the acetowhite effect is weak. For this reason, the acetowhite effect is typically observed in the 540 to 580 nm region (green region) where hemoglobin provides strong absorption in the stroma; conversely, it is barely observed at wavelengths longer than 600 nm (red region) where hemoglobin absorption is low.<sup>5,6,8,14</sup>

Figure 2 also shows that variations in the actual epithelium thickness do not have a strong effect on the reflectance observed. Epithelium thickness values shown in Fig. 2 represent minimum, average, and maximum values for the epithelium of the human cervix, as reported in Ref. 11. Effects of epithelium layer thickness can be modeled and taken into account, but because they do not appear to drastically affect the total reflectance all subsequent simulations and results in this first attempt to model the acetowhite effect refer to the average epithelium thickness of 0.36 mm.



**Fig. 2** Reflectance for CIN3 lesions calculated using MC simulations (data points) for three different thickness values ( $z$ ) of the epithelium layer. The scattering coefficient of the stroma layer was assumed equal to  $1.6 \text{ mm}^{-1}$  in all three cases. Solid lines represent spline fits to the MC data points.

Another parameter that is subject to biological variability, and affects the total reflectance, is the reduced-scattering coefficient in the stroma layer. For all simulations reported in Fig. 2, the reduced-scattering coefficient of the stroma layer was assumed fixed at  $1.6 \text{ mm}^{-1}$  which is a reasonable value for this type of tissue in the visible and NIR wavelength regions.<sup>13</sup> To assess the effect of variations in the reduced-scattering



**Fig. 3** Reflectance for CIN3 lesions calculated using MC simulations (data points) for three different values of the reduced-scattering coefficient of the stroma layer. Epithelial layer thickness was  $z = 0.36$  mm in all three cases. Solid lines represent spline fits to the MC data points.

coefficient of the stroma in the total observed reflectance, the reduced-scattering coefficient of the stroma layer was varied in the  $1.0$  to  $2.0$   $\text{mm}^{-1}$  range. Typical simulation results are shown in Fig. 3, illustrating that variations in the reduced-scattering coefficient of the stroma do not appear to drastically affect the total observed reflectance. Because of this observation (just as in the case of epithelium layer thickness) all subsequent

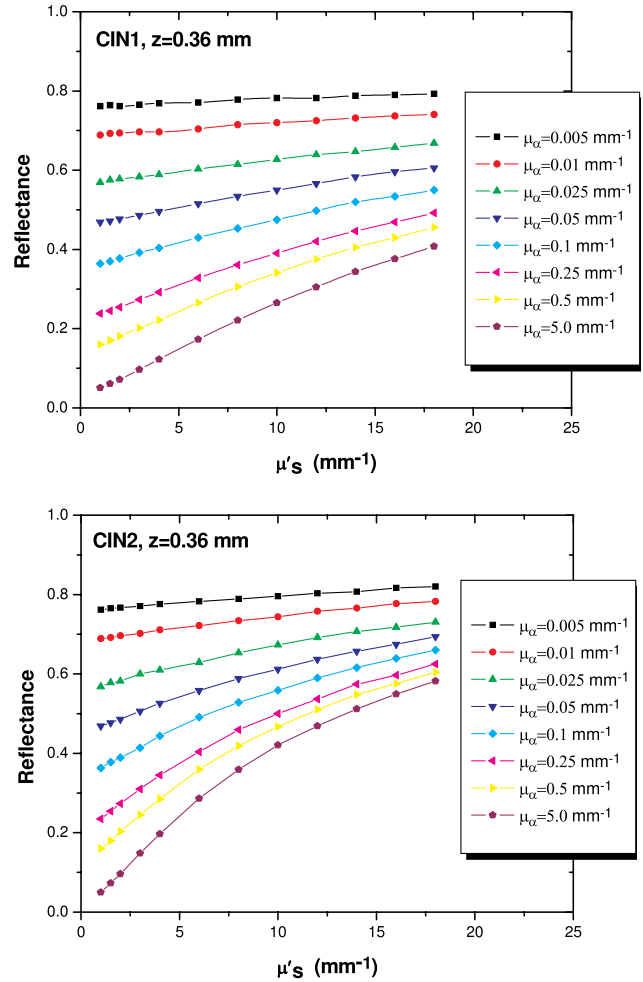


**Fig. 4** Reflectance for CIN1 and CIN2 lesions calculated using MC simulations (data points). Solid lines represent spline fits to the MC data points.

simulations and results refer to a typical value of the stroma reduced-scattering coefficient of  $1.6$   $\text{mm}^{-1}$ .

Figure 4 shows simulation results for CIN1 and CIN2 lesions. These were implemented using the three-layer geometry outlined in the methods section. Reflectance results for these two lesion types generally exhibit the main feature of the CIN3 lesions, i.e., stroma absorption is important for the observation of the acetowhite effect. In addition, the thickness of the dysplastic cell layer in the epithelium also appears important with CIN1 lesions exhibiting a weaker version of the acetowhite effect than CIN2 lesions, which, in turn, exhibit a weaker acetowhite effect than CIN3 lesions.

To describe the acetowhite effect in a quantitative way, the ratio of the reflectance at the highest and lowest values of the reduced-scattering coefficient was used:

$$S = R(\mu'_s = 18 \text{ mm}^{-1})/R(\mu'_s = 1.0 \text{ mm}^{-1}). \quad (1)$$

This ratio,  $S$ , termed “acetowhite sensitivity,” is a quantitative measure of the increase in reflectance due to the acetowhite effect and is presented in Fig. 5 using the data shown in Figs. 2 to 4. In Fig. 5(a), the acetowhite sensitivity is shown for three different thickness values of the epithelium layer for

CIN3. In general, the thicker the epithelium the stronger the acetowhite effect is, with the exception of large stroma absorption where a thinner acetowhite epithelium produces stronger acetowhite effect. Figure 5(b) shows the effect of the stroma reduced-scattering coefficient on the acetowhite effect, illustrating that lower stroma scattering produces stronger acetowhite effect. Finally, Fig. 5(c) shows the acetowhite effect for three representative cases of CIN1, CIN2, and CIN3. As can be seen, CIN3 produces the stronger acetowhite effect, as expected, but CIN2 is remarkably close to CIN3, while CIN1 is characterized by clearly smaller acetowhite effect. This similarity between CIN2 and CIN3 is remarkable because histologically they are also closer, compared to CIN1. Figure 5 illustrates that when stroma absorption is minimal, the acetowhite effect is weak (corresponding to only about 10% increase in reflectance) while for stronger stroma absorption, the acetowhite effect becomes much more pronounced, yielding up to an entire order of magnitude increase in reflectance.

Using the MC reflectance results, it is now possible to construct semi-empirical analytical models that describe the MC data and carry all the advantages and convenience of an analytical expression. To model CIN1, the MC data shown in Fig. 4 were used. It was found, using methods described in Sec. 2.2, that the data can be described by Eq. (2),

$$R = \frac{1}{a_1 + b_1\mu_a + c_1\sqrt{\mu_a}} + \frac{\sqrt{\mu'_s} \ln \mu'_s}{a_2 + b_2 \ln \mu_a/\mu_a + c_2/\mu_a}, \quad (2)$$

that includes six empirical parameters (determined during the fitting process) summarized in Table 4. In Eq. (2),  $\mu_a$  is the absorption coefficient of the stroma layer and  $\mu'_s$  is the reduced-scattering coefficient of the epithelium layer. The fit of Eq. (2) to the MC data is shown in Fig. 6 illustrating the fact that Eq. (2) describes the MC data well.

To model CIN3, the MC data shown in Fig. 2 were used corresponding to the average epithelium thickness ( $z = 0.36$ ). In this case, Eq. (3) was found to describe the data well.

$$R = a_1 + b_1(1 + c_1\mu_a)^{-1/2} + (e^{a_2+b_2(\ln \mu_a)^2+c_2\sqrt{\mu_a}})\sqrt{\mu'_s}. \quad (3)$$

The fit of Eq. (3) to the MC data is shown in Fig. 7. Just as in the case of Eq. (2), Eq. (3), includes six empirically determined parameters that are summarized in Table 4;  $\mu_a$  is the absorption coefficient of the stroma layer and  $\mu'_s$  is the reduced-scattering coefficient of epithelium layer. Typical  $r^2$  values for the fits shown in Figs. 6 and 7 are better than 0.99.

It is now possible to proceed to analyze actual experimental reflectance data of the acetowhite effect in CIN lesions of the cervix reported in Ref. 6. Note that a model for CIN2 was not explicitly developed because no CIN2 reflectance data are reported in Ref. 6 but they are combined with CIN3 because they are both generally considered precancerous lesions compared to CIN1 lesions, which are generally considered benign. Thus, clinically, it is useful and important to be able to distinguish between CIN1 and CIN2/CIN3 lesions rather than between CIN2 and CIN3. Nevertheless, it should be pointed out that a model for CIN2 can be easily developed. Just as in the case of CIN1 and CIN3, Eqs. (2) and (3) or a variation of these may be found suitable to describe the data using techniques similar to those described earlier in the methods section.

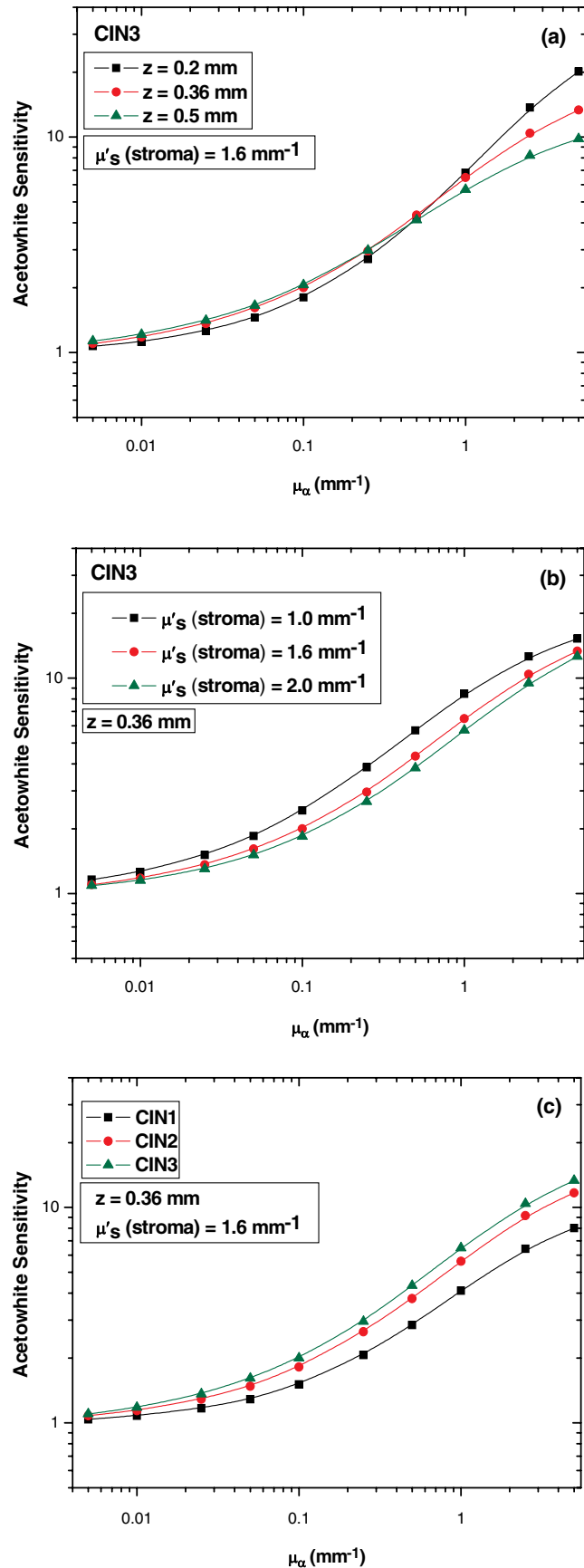
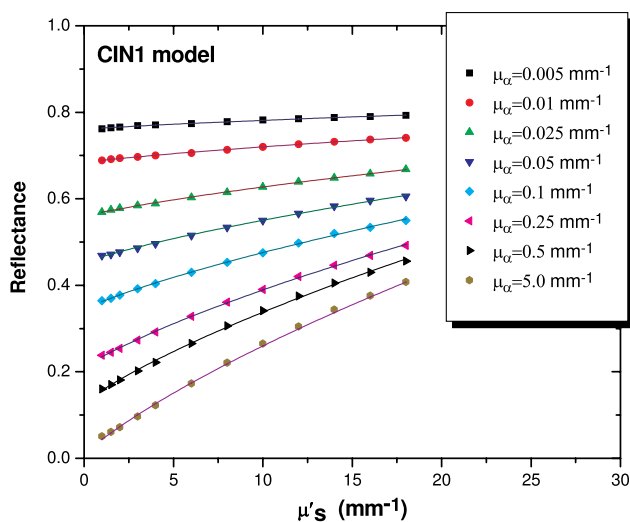


Fig. 5 Acetowhite sensitivity [Eq. (1)] in various cases using the data shown in Figs. 2 to 4. Solid lines represent spline interpolation between data points.



**Fig. 6** Reflectance model for CIN1 lesions. Same MC reflectance data shown in Fig. 4(a). Solid lines represent model fits to Eq. (2).

For the purposes of our further analysis, we will make the assumption that the model developed for CIN3 is approximately suitable for analysis of CIN2 data that are potentially reported combined with CIN3 in Ref. 6.

Figure 8 shows the reduced-scattering coefficient calculated using the model of Eq. (3) for three typical CIN3 lesions reported in Fig. 4(d) in Ref. 6. The increase in the scattering coefficient of the epithelium due to the acetowhite effect is within an order of magnitude. Figure 9 shows a similar calculation of the reduced-scattering coefficient of the epithelium in CIN3 lesions using two different acetic acid concentrations (3% and 5%) [data from Fig. 6(b) in Ref. 6]. Note that the difference in the reduced-scattering coefficient of the epithelium is almost twofold between the two different concentrations, in contrast to the difference in reflectance, which is quite smaller. This observation is in agreement with the findings of the modeling work presented by Balas et al.<sup>6</sup> In their work, they generally attribute the smaller difference observed in reflectance to light-scattering effects; in the present work the analytical model employed offers an interesting direct quantitative confirmation to their qualitative prediction.

Finally, Fig. 10 shows the reduced-scattering coefficient, calculated using the model of Eq. (2), for three typical CIN1 lesions reported in Fig. 4(c) in Ref. 6. Just as in the case of high grade lesions (CIN2/3) an increase is observed in the reduced-scattering coefficient of the epithelium due to the acetowhite effect. Note that the overall increase in the reduced-scattering coefficient of the epithelium is smaller, as expected in CIN1 lesions.

It is worth noting that the reduced-scattering coefficient shown in Figs. 8 to 10 does not strongly depend on the actual value of the stroma absorption coefficient. As can be seen from Figs. 2 to 4, the absorption coefficient varies in a range spanning three orders of magnitude while the reduced-scattering coefficient varies correspondingly by only one order of magnitude. This confirms that the reduced-scattering coefficient is not particularly sensitive to small variations in the absorption coefficient. Even though there is no standard way to quantitatively describe this sensitivity, a quantitative example is also presented in support of the above observation: a 100% increase in the

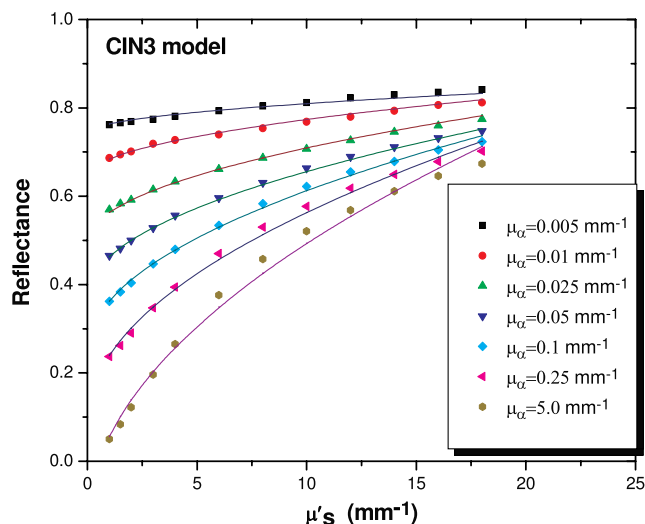


**Fig. 7** Reflectance model for CIN3 lesions. Same MC reflectance data shown in Fig. 2 ( $z = 0.36$  mm). Solid lines represent model fits to Eq. (3).

stroma absorption coefficient (from 0.08 to 0.16  $\text{mm}^{-1}$ ) results in only 20% error in the estimation of the reduced-scattering coefficient of the epithelium (from 10 to 12  $\text{mm}^{-1}$ ). Similar arguments hold for the epithelium baseline reduced-scattering coefficient that may typically vary as  $1.5 \pm 0.5 \text{ mm}^{-1}$  while the actual reduced-scattering coefficient varies by an order of magnitude in contrast.

In all data analysis shown in Figs. (8) to (10), the absorption coefficient of the stroma layer was calculated using the initial reflectance value at  $t = 0$  by assuming an initial epithelial reduced-scattering coefficient equal to 1.0  $\text{mm}^{-1}$  and numerically solving Eqs. (2) and (3) for the stroma absorption coefficient. The actual absorption coefficient values are reported in Figs. 8(b), 9(b), and 10(b). Following determination of the stroma absorption coefficient, Eqs. (2) and (3) were also numerically solved to obtain the epithelium reduced-scattering coefficient at each time point. Continuous lines in Figs. 8 to 10 represent spline interpolation between data points.

## 4 Discussion

Even though the acetowhite effect has been studied *in vivo* in several studies utilizing imaging, as well as spectral imaging techniques,<sup>4-10</sup> no detailed reflectance model has been presented yet (to the author's knowledge). Such a quantitative reflectance model is presented in this article, describing key features of the acetowhite effect that can be summarized as follows.

- (1) The acetowhite effect can be modeled by assuming a transient change in the scattering properties of the epithelium layer. The reduced-scattering coefficient of the dysplastic epithelium typically increases by an order of magnitude due to application of dilute (3% to 5%) acetic acid solution.
- (2) The absorption of the epithelium layer can be reasonably assumed to be negligible (assumption realistic in the visible and near-infrared regions) but the absorption of the stroma layer immediately below is crucial for the observation of the acetowhite effect using common imaging techniques during

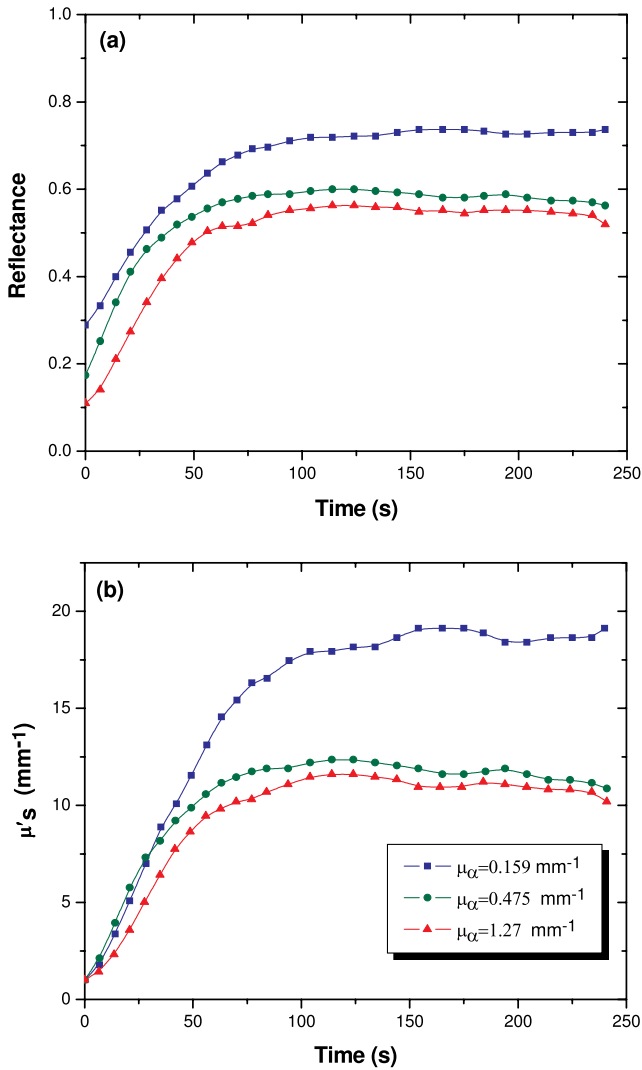


**Fig. 8** (a) Experimental reflectance data demonstrating the acetowhite effect for three different CIN3 lesions in the cervix (data from Ref. 6). (b) Corresponding values of the reduced-scattering coefficient of the epithelium calculated using the model [Eq. (3)].

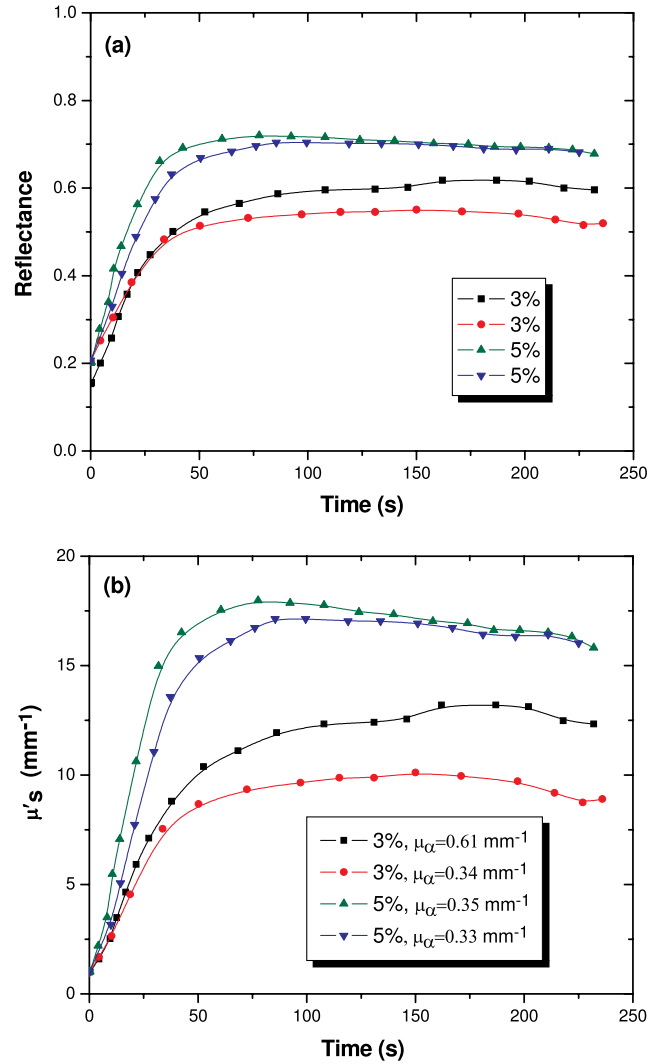


**Fig. 9** Experimental reflectance data demonstrating the acetowhite effect for four different CIN3 lesions in the cervix, two using 3% acetic acid solution and two using 5% acetic acid solution (data from Ref. 6). (b) Corresponding values of the reduced-scattering coefficient of the epithelium calculated using the model [Eq. (3)].

colposcopy. If the absorption coefficient in the stroma layer is negligible, then the acetowhite effect is weak, regardless of the significant increase in the reduced-scattering coefficient in the epithelium. This characteristic has been previously observed experimentally<sup>5,6,8,14</sup> using spectral imaging in the 540 to 580 nm range where hemoglobin absorption in the stroma layer is higher. In contrast, at wavelengths longer than 600 nm, where hemoglobin absorption is low, the acetowhite effect is significantly diminished. The model presented in this article offers a quantitative explanation for this interesting and important characteristic of the acetowhite effect. It is important to keep in mind that this observation is valid for the typical imaging delivery/collection geometry employed in colposcopy.<sup>5,6,8</sup>

- (3) The exact thickness of the epithelium layer (which typically varies in the 0.2 to 0.5 mm range with

**Table 4** Parameter values used in Eqs. (2) and (3).

	$a_1$	$b_1$	$c_1$	$a_2$	$b_2$	$c_2$
Eq. (2)	0.9697	3.819	4.462	32.33	0.5184	4.331
Eq. (3)	-0.2282	1.046	40.32	-1.877	-0.06523	0.2001

an average thickness of 0.36 mm in the cervix), also affects the reflectance measured. This effect is generally small compared to the effect of the absorption coefficient of the stroma layer. Similarly, the exact value of the reduced-scattering coefficient in the stroma layer, which may vary typically in the 1.0 to 2.0 mm<sup>-1</sup> range (visible and NIR spectral regions), does not appear to affect the reflectance greatly either.

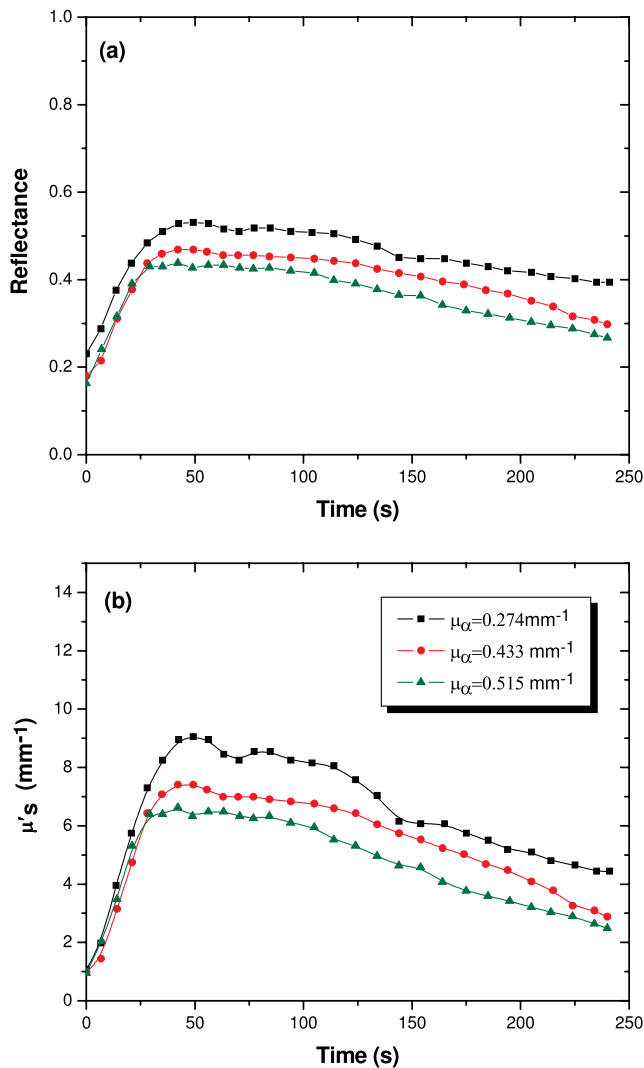


**Fig. 10** (a) Experimental reflectance data demonstrating the acetowhite effect for three different CIN1 lesions in the cervix (data from Ref. 6). (b) Corresponding values of the reduced-scattering coefficient of the epithelium calculated using the model [Eq. (2)].

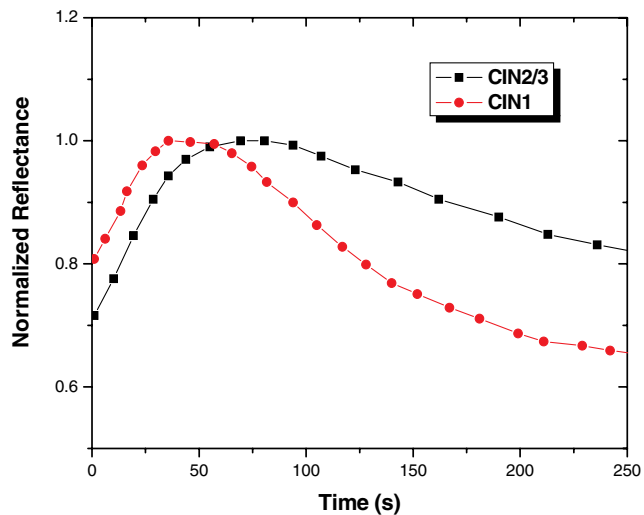


**Fig. 11** Average experimental reflectance data for the acetowhite effect in CIN1 and CIN2/3 lesions (data from Ref. 10) illustrating the weaker, on average, acetowhite effect in CIN1 lesions.

In addition, several other observations are worth mentioning. Balas et al.<sup>6</sup> predict an almost two-fold increase in epithelial scattering due to application of 5% acetic acid solution as opposed to 3% solution. This change is not observed in their experimental reflectance data, but by observing the actual differences in the values of the reduced-scattering coefficient calculated using the model presented in this article. These are found to be much more consistent with the predictions of Balas et al.<sup>6</sup>

For CIN1 lesions, the model predicts lower reflectance than CIN2 and CIN3 lesions. This is due to the fact that epithelial cells associated with the acetowhite effect are located deeper in the CIN1 epithelium. This is immediately evident by inspection of Figs. 2 and 4. This particular feature is also due to the fact that dysplastic cells exhibiting the acetowhite effect are limited to a thinner layer of the epithelium as opposed to CIN2 and CIN3. Apart from the data reported in Ref. 6 and analyzed here, the expected smaller variation in the reflectance change due to the acetowhite effect is also evident in the data reported by Wu et al.<sup>10</sup> These data are shown in Fig. 11 illustrating a smaller dynamic range for reflectance (from  $t = 0$  up until peak reflectance time point) and they are consistent with the predictions of the model presented above.

For CIN2 lesions no detailed quantitative model has been presented (as in the case of CIN1 and CIN3). This is because no CIN2 reflectance data are presented in Ref. 6 but are instead combined together with CIN3. Data are combined, because both CIN2 and CIN3 are potentially precancerous and are classified together by pathologists. However, a reflectance model can be easily obtained for CIN2 by finding an empirical fit to the data shown in Fig. 4 in a manner analogous to CIN1 and CIN3. In fact, assuming all other optical properties are similar, the model would predict lower reflectance for CIN2 than CIN3 and higher than CIN1. This would be interesting to study in actual CIN2 data. Preliminary data published previously in Refs. 4 and 5 are consistent with the model predictions presented here.

It is important to keep in mind that the acetowhite effect is a transient effect and that the model presented here does not deal with the changes of epithelial scattering versus time, but rather with the changes of epithelial reflectance versus epithelial scattering. Combination of the two modeling approaches, in future work, may produce more accurate and useful diagnostic algorithms based on the acetowhite effect.

The model presented here, is meant to be a first approximate model to describe basic features of the acetowhite effect in a quantitative manner. In that spirit, no attempt was made to model in detail parameters such as epithelial layer thickness and scattering in the stroma. In addition, no attempt was made to apply the model in a diagnostic way, such as using the model for algorithm development to discriminate between CIN1 and CIN2/3 lesions. These are all very interesting future modeling tasks, together with more accurate and rigorous validation and tuning of the model on epithelial tissue phantoms.

Another important point that needs to be stressed is that the current formulation of the semi-empirical model [Eqs. (2) and (3)] is distinctly different for CIN1 and CIN3. It would be great if one could come up with a single-expression model for all three stages of CIN. However, it is not immediately clear if this is possible. CIN1 and CIN2 constitute a three-layer problem, while CIN3 is a two-layer problem. Perhaps CIN3 could be modeled as a limiting case of a three-layer problem, but it is not obvious what that three-layer analytical model expression would be. This is an open question for future investigations.

Finally, it must be stressed that much remains unknown regarding the exact microscopic origins of the acetowhite effect and the resulting changes in the scattering properties of the epithelium. More detailed knowledge about these, which may become available in the future, will greatly facilitate the development of better reflectance models for the description of the acetowhite effect.

### Acknowledgments

The author would like to thank Costas Balas for several useful discussions.

### References

1. R. Lambert, J. F. Rey, and R. Sankaranarayanan, "Magnification and chromoscopy with the acetic acid test," *Endoscopy* **35**(5), 437–445 (2003).
2. A. B. MacLean, "Acetowhite epithelium," *Gynecol. Oncol.* **95**(3), 691–694 (2004).
3. N. Thekkek and R. Richards-Kortum, "Optical imaging for cervical cancer detection: solutions for a continuing global problem," *Nat. Rev. Cancer* **8**(9), 725–731 (2008).
4. C. J. Balas et al., "In vivo detection and staging of epithelial dysplasias and malignancies based on the quantitative assessment of acetic acid-tissue interaction kinetics," *J. Photochem. Photobiol.B* **53**(1–3), 153–157 (1999).
5. C. Balas, "A novel optical imaging method for the early detection, quantitative grading, and mapping of cancerous and precancerous lesions of cervix," *IEEE Trans. Biomed. Eng.* **48**(1), 96–104 (2001).
6. C. Balas, G. Papoutsoglou, and A. Potirakis, "In vivo molecular imaging of cervical neoplasia using acetic acid as biomarker," *IEEE J. Quant. Electron.* **14**(1), 29–42 (2008).
7. B. W. Pogue, M. A. Mycek, and D. Harper, "Image analysis for discrimination of cervical neoplasia," *J. Biomed. Opt.* **5**(1), 72–82 (2000).
8. B. W. Pogue et al., "Analysis of acetic acid-induced whitening of high-grade squamous intraepithelial lesions," *J. Biomed. Opt.* **6**(4), 397–403 (2001).
9. W. Li et al., "Using acetowhite opacity index for detecting cervical intraepithelial neoplasia," *J. Biomed. Opt.* **14**(1), 014020 (2009).
10. T. Wu et al., "Clinical study of quantitative diagnosis of early cervical cancer based on the classification of acetowhitening kinetics," *J. Biomed. Opt.* **15**(2), 026001 (2010).
11. D. C. Walker et al., "A study of the morphological parameters of cervical squamous epithelium," *Physiol. Meas.* **24**(1), 121–135 (2003).
12. L. H. Wang, S. L. Jacques, and L. Q. Zheng, "MCML—Monte Carlo modeling of light transport in multilayered tissues," *Comput. Methods Programs. Biomed.* **47**(2), 131–146 (1995).
13. T. Collier et al., "Sources of scattering in cervical tissue: determination of the scattering coefficient by confocal microscopy," *Appl. Opt.* **44**(11), 2072–2081 (2005).
14. S. Y. Park et al., "Automated image analysis of digital colposcopy for the detection of cervical neoplasia," *J. Biomed. Opt.* **13**(1), 014029 (2008).